

## In-beam $\gamma$ -ray spectroscopy and inclusive two-proton knockout cross section measurements at $N \approx 40$

P. Adrich,<sup>1,\*</sup> A. M. Amthor,<sup>1,2</sup> D. Bazin,<sup>1</sup> M. D. Bowen,<sup>1,2</sup> B. A. Brown,<sup>1,2</sup> C. M. Campbell,<sup>1,2</sup> J. M. Cook,<sup>1,2</sup> A. Gade,<sup>1,2</sup> D. Galaviz,<sup>1</sup> T. Glasmacher,<sup>1,2</sup> S. McDaniel,<sup>1,2</sup> D. Miller,<sup>1,2</sup> A. Obertelli,<sup>1</sup> Y. Shimbara,<sup>1</sup> K. P. Siwek,<sup>1,2</sup> J. A. Tostevin,<sup>3</sup> and D. Weisshaar<sup>1</sup>

<sup>1</sup>National Superconducting Cyclotron Laboratory, Michigan State University, East Lansing, Michigan 48824, USA

<sup>2</sup>Department of Physics and Astronomy, Michigan State University, East Lansing, Michigan 48824, USA

<sup>3</sup>Department of Physics, Faculty of Engineering and Physical Sciences, University of Surrey, Guildford, Surrey GU2 7XH, United Kingdom

(Received 16 November 2007; revised manuscript received 22 February 2008; published 9 May 2008)

In-beam  $\gamma$ -ray spectroscopy of  $^{66,68}\text{Fe}$  following intermediate-energy one- and two-proton knockout from cobalt and nickel secondary beams has been performed at the National Superconducting Cyclotron Laboratory. New transitions have been observed in  $^{66}\text{Fe}$  and  $^{68}\text{Fe}$ . This is the first observation of  $\gamma$ -ray transitions in  $^{68}\text{Fe}$ . In addition,  $^{64}\text{Cr}$  was produced using the  $^9\text{Be}(^{66}\text{Fe}, ^{64}\text{Cr})\text{X}$  two-proton knockout reaction. An unexpectedly low inclusive cross section is observed for this reaction, an order of magnitude smaller than for the  $^9\text{Be}(^{68}\text{Ni}, ^{66}\text{Fe})\text{X}$  reaction. This observation is discussed in terms of a significant structural difference between  $^{66}\text{Fe}$  and  $^{64}\text{Cr}$  and considerable admixtures of  $\nu(pf)^{n-2}(g_{9/2})^{+2}$  configurations in the ground and excited states of  $^{64}\text{Cr}$  at  $N = 40$ .

DOI: 10.1103/PhysRevC.77.054306

PACS number(s): 23.20.Lv, 27.50.+e, 24.50.+g, 25.60.-t

### I. INTRODUCTION

Shell closures form the cornerstones of models that describe the structure of the atomic nucleus. In exotic nuclei with extreme ratios of  $N/Z$ , the shell structure as established for stable nuclei is modified: “classic” magic numbers break down and new shell gaps develop (e.g., Refs. [1–4]).

A prime example of the modification of a *canonical* magic number is the so-called *island of inversion* near  $^{31}\text{Na}$  at  $N \approx 20$  [5–8]. Contrary to the predominantly spherical shape of stable nuclei with magic or close to magic numbers of protons or neutrons, nuclei in the island of inversion assume deformed shapes in their ground states (g.s.). In a microscopical picture this is explained by the dominance of the deformation driving  $\nu(sd)^{-2}(fp)^{+2}$  particle-hole intruder configurations ( $2\hbar\omega$  excitations across the  $N = 20$  shell gap) in the ground- and low-energy excited states. The existence of the *island of inversion* is possible due to a reduction of the *sd-fp* shell gap caused by the tensor force [2,8].

The tensor force has been shown to influence the shell structure in a unique and robust way throughout the nuclear chart [2,9]. Similarly to the island of inversion near  $^{31}\text{Na}$  a characteristic shell evolution is expected in the region of nuclei with protons in the  $f_{7/2}$  orbit and a closed or nearly closed neutron *pf* shell, i.e., for the  $N \approx 40$  isotones between Ca and Ni. The attractive monopole part of the tensor force, acting between  $\pi f_{7/2}$  protons and  $\nu f_{5/2}$  neutrons, is weakened as protons are removed from the  $\pi f_{7/2}$  orbital when going from nickel toward calcium, and in effect, the  $\nu f_{5/2}$  orbit shifts up in energy. As a result, the gap between the  $\nu f_{5/2}$  and  $\nu g_{9/2}$  orbits, which is already rather small in  $^{68}\text{Ni}$  [10,11], is expected to be further reduced, provoking neutron pair scattering to the intruder  $\nu g_{9/2}$  orbit already for nuclei with fewer than 40 neutrons. In analogy to  $Z \approx 11$ ,  $N \approx 20$  nuclei, the

existence of a new island of inversion in the region of  $N \approx 40$  isotopes of Cr and Ti has been suggested [3,12,13]. The arguments are, however, rather qualitative as theoretical calculations in this region face difficulties related to the large dimension of the necessary model space and the lack of reliable effective interactions.

On the experimental side the growing body of data suggests an increasing importance of the  $\nu g_{9/2}$  orbital for  $N \approx 40$ ,  $\pi f_{7/2}$  nuclei [10,14–23]. In particular, energies of the first excited  $2^+$  states measured in even-even iron and chromium isotopes (see Fig. 1) exhibit a decreasing trend toward  $N = 40$ , which is often interpreted in terms of an onset of deformation. The nucleus  $^{64}\text{Cr}$  with  $Z = 24$  and  $N = 40$  is expected to be the most deformed in the region and thus to exhibit the lowest  $E(2^+)$  energy [13,15].

### II. EXPERIMENT

In the present work we report on the  $\gamma$ -ray spectroscopy of neutron-rich,  $N \approx 40$ , iron isotopes and on inclusive two-proton knockout cross section for reactions in this region. The experiment was carried out at the National Superconducting Cyclotron Laboratory (NSCL) at Michigan State University. A primary beam of  $^{76}\text{Ge}$  was accelerated to an energy of 130 MeV/nucleon by the Coupled Cyclotron Facility (CCF) and fragmented in a 470-mg/cm<sup>2</sup>-thick  $^9\text{Be}$  target. Projectile fragments were then separated in the A1900 fragment separator using the  $B\rho$ - $\Delta E$ - $B\rho$  method [24]. The resulting cocktail beam was delivered to the target position of the S800 spectrograph [25] where a secondary  $^9\text{Be}$  target was located. Several different settings of the A1900 separator optimized to maximize the intensities of  $^{66}\text{Fe}$ ,  $^{67}\text{Co}$ ,  $^{69}\text{Co}$ ,  $^{68}\text{Ni}$ , and  $^{70}\text{Ni}$  beams were used during the experiment. The momentum acceptance of the A1900 was restricted to 1% for all settings except for the  $^{66}\text{Fe}$  and  $^{70}\text{Ni}$  projectiles for which it was increased to 2%. The resulting cocktail beams were

\*adrich@nscl.msu.edu

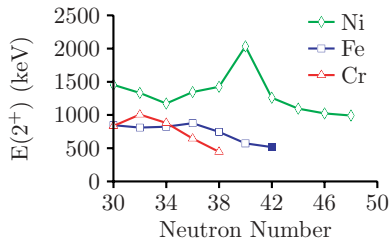


FIG. 1. (Color online) Systematics of experimental energies of the first excited states in even-even isotopes of nickel ( $Z = 28$ ; diamond), iron ( $Z = 26$ ; square), and chromium ( $Z = 24$ ; triangle). Full symbol represents data first obtained in this work.

typically composed of two or three isotopes of similar mass to charge ( $A/Q$ ) ratio and comparable intensities and a number of contaminants transported with much lesser intensities. The purities of the secondary beams were 33% for  $^{66}\text{Fe}$ , 84% for  $^{67}\text{Co}$ , 17% for  $^{69}\text{Co}$ , 52% for  $^{68}\text{Ni}$ , and 6% for  $^{70}\text{Ni}$  beam. Different components of the cocktail beam were identified event by event by means of the time-of-flight measured with a pair of thin plastic scintillators located before the target.

$^{68}\text{Ni}$  is known to have an isomeric first excited  $0^+$  state with  $t_{1/2} = 270$  ns that can decay only by internal conversion. The projectiles in our experiment are available as fully stripped ions and the decay by conversion electron is, to first order, strongly hindered. For example, the isomeric content of the  $^{68}\text{Ni}$  secondary beam from the first excited  $0^+$  state and from the  $5^-$ ,  $t_{1/2} = 0.86$  ms isomer were measured in an experiment at GANIL [10] to be  $<2\%$  and 18(5)%, respectively. In that experiment the  $^{68}\text{Ni}$  secondary beam was produced from fragmentation of  $^{70}\text{Zn}$  on a  $^{58}\text{Ni}$  target at about 66 MeV/nucleon. In the current experiment, it was not possible to measure the isomeric content of the secondary beams. Because the mechanisms of isomer population in fragmentation reactions are not understood, it is impossible to estimate the isomeric content of the secondary  $^{68}\text{Ni}$  beam used in the current experiment. It could, however, have been different from the GANIL experiment cited above, because a different combination of primary beam, target, and beam energy was used.

The projectile-like residues produced from reactions in the secondary target were transported to the S800 focal plane, where they were identified event by event from the energy loss measured in an ionization chamber and the time-of-flight measured with plastic scintillators between the object position and the focal plane of the S800. One-proton knockout reactions from  $^{67}\text{Co}$  and  $^{69}\text{Co}$  projectile beams and two-proton knockout reactions from  $^{68}\text{Ni}$ ,  $^{70}\text{Ni}$ , and  $^{66}\text{Fe}$  beams were studied in five separate runs. For each run the S800 spectrograph was set to accept the projectile-like knockout residue of interest. The secondary reaction target thickness was  $376$  mg/cm $^2$  for the  $^{66}\text{Fe}$  run and  $188$  mg/cm $^2$  for all other runs. The mean midtarget energy of the projectile was 73.5 MeV/nucleon for  $^{66}\text{Fe}$ , 84.3 MeV/nucleon for  $^{67}\text{Co}$ , 77.8 MeV/nucleon for  $^{69}\text{Co}$ , 74.7 MeV/nucleon for  $^{68}\text{Ni}$ , and 71.8 MeV/nucleon for  $^{70}\text{Ni}$ .

Examples of particle identification plots are shown in Fig. 2. The upper panel shows a composition of the secondary

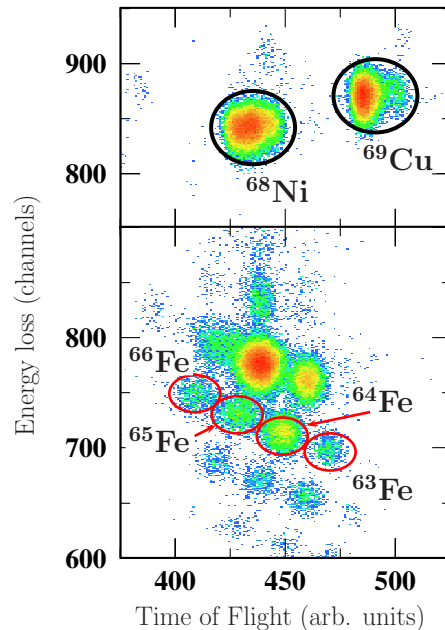


FIG. 2. (Color online) (Upper panel) Example of particle identification of the secondary cocktail beam impinging onto the reaction target. The secondary cocktail beam results from fragmentation of primary  $^{76}\text{Ge}$ . In the case illustrated here the A1900 fragment separator was optimized for transmission of  $^{68}\text{Ni}$  fragments. (Lower panel) Identification of reaction residues in the S800 resulting from the  $^{68}\text{Ni}$  secondary beam interacting with the  $^9\text{Be}$  reaction target.

cocktail beam produced in the A1900 and optimized for  $^{68}\text{Ni}$ . It was obtained by matching the magnetic rigidity setting of the S800 spectrograph to the rigidity of the  $^{68}\text{Ni}$  beam taking into account energy loss in the secondary target. Such measurements were done for all projectile beams and served as normalizations for the subsequent measurements of the reaction cross sections.

The lower panel of Fig. 2 shows the identification of reaction residues. In the example shown, the field of the S800 spectrograph was set to match the magnetic rigidity of the  $^{66}\text{Fe}$  residue produced in the two-proton knockout reaction from  $^{68}\text{Ni}$  projectile. Because of the large acceptance of the spectrograph, a number of other isotopes, produced in a variety of reaction channels, were transmitted to the focal plane at the same time.

Inclusive cross sections for two-proton knockout reactions were derived from the yields of projectile-like residues detected at the S800 focal plane and the number of incoming projectile ions, taking into account the thickness of the secondary target. Systematic uncertainties arising from particle identification (5%), stability and purity of the beam (5%), and homogeneity of the target thickness (0.5%) were added to the statistical uncertainty in quadrature.

Prompt  $\gamma$ -ray emission from excited reaction residues was measured with SeGA, an array of 32-fold segmented high-purity germanium (HPGe) detectors [26]. The array was set up around the target in two rings with seven detectors at  $37^\circ$  and nine detectors at  $90^\circ$  relative to the beam axis. The total energy deposited in a HPGe crystal is readout

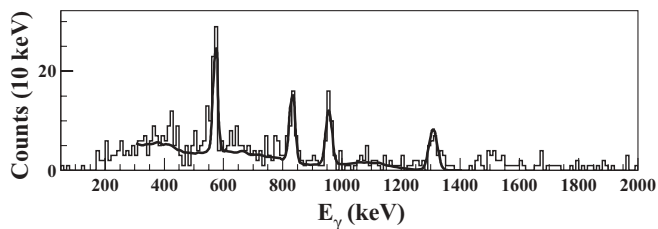


FIG. 3. GEANT-simulated response (thick, solid line) superimposed on the  $\gamma$ -ray spectrum measured in coincidence with  $^{66}\text{Fe}$  fragments produced in the  $^9\text{Be}(^{67}\text{Co}, ^{66}\text{Fe})\text{X}$  reaction.

by the central electrode while signals induced in the outer (segmented) electrodes are used to determine the point of first interaction (which is assumed to be in the center of a segment with the highest energy deposit). The energy of the detected  $\gamma$  ray is then event-by-event Doppler corrected to the projectile frame ( $v \approx 0.37c$ ), taking advantage of the interaction position deduced from the segment information.

The total photopeak efficiency of the array was measured with calibration sources located at the target position and amounts to 2% at 1 MeV. GEANT3 [27] simulations successfully modeled the efficiency of the array and provided the detector response for in-beam data by taking into account the Lorentz boost arising from the velocity of the reaction residues at the moment of the  $\gamma$ -ray emission ( $v/c$  around 0.37). Figure 3 shows a scaled, GEANT-simulated response superimposed on the  $\gamma$ -ray spectrum measured in coincidence with  $^{66}\text{Fe}$  fragments produced in  $^9\text{Be}(^{67}\text{Co}, ^{66}\text{Fe})\text{X}$  reaction. Due to the coincidence condition imposed on the  $\gamma$ -rays detected in SeGA and heavy ions measured at the S800 focal plane, the resulting  $\gamma$ -ray spectra feature very little background.

Main sources of systematic errors on the reconstructed energies are associated with the uncertainty in the exact target location relative to the center of the SeGA array and with the uncertainty in the mean velocity of the reaction residues. The total systematic error on the energy of the  $\gamma$ -ray transition is on the order of 1%, whereas the energy resolution is 2–3% (full width at half maximum) at 1 MeV depending on the momentum spread of the beam and the target thickness.

### III. RESULTS AND DISCUSSION

In the first part of the experiment the in-beam  $\gamma$ -ray spectroscopy of  $^{66}\text{Fe}$  and  $^{68}\text{Fe}$  was studied. In Fig. 4 we present Doppler-corrected  $\gamma$ -ray spectra measured in coincidence with  $^{66}\text{Fe}$  and  $^{68}\text{Fe}$  residues produced in two reactions: by one-proton knockout from  $^{67}\text{Co}$  and  $^{69}\text{Co}$ , respectively, and by two-proton knockout from  $^{68}\text{Ni}$  and  $^{70}\text{Ni}$ , respectively.

#### A. $^{66}\text{Fe}$

The  $\gamma$ -ray spectra measured in coincidence with  $^{66}\text{Fe}$  residues display three strong peaks. In the one-proton knockout reaction the centroids of these peaks are 571(6), 833(9), and 957(10) keV and in two-proton knockout the centroids are 567(6), 832(9), and 957(10) keV. Within experimental

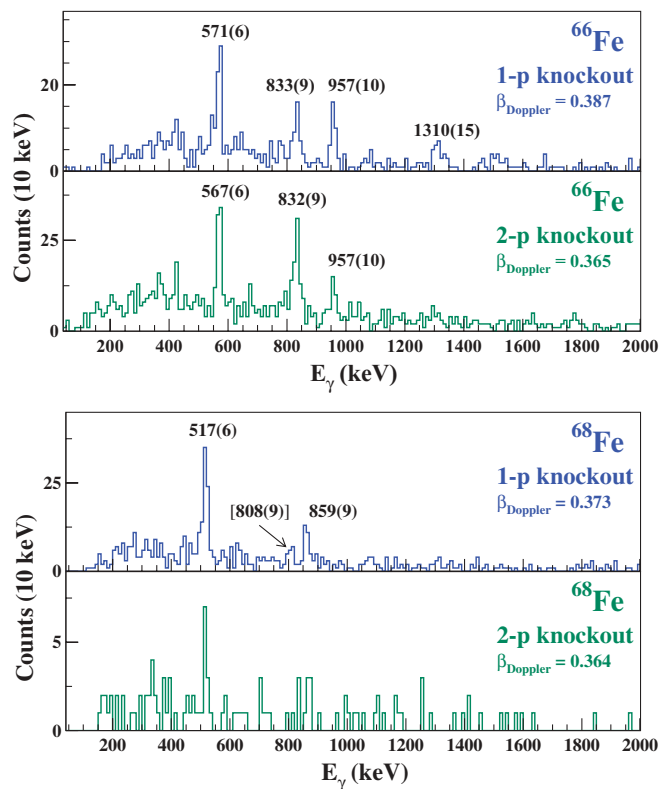


FIG. 4. (Color online) Doppler-corrected  $\gamma$  ray energy spectra measured in coincidence with  $^{66}\text{Fe}$  (two top panels) and  $^{68}\text{Fe}$  (two bottom panels) projectile-like residues. The reaction used to produce given residue and velocity used for Doppler correction are indicated in each panel. The peak centroids are indicated (in units of keV) together with their experimental uncertainties.

uncertainties the peaks observed in both spectra have the same centroids and thus we assume they correspond to the same transitions. In addition, in the one-proton knockout channel we observe a weak transition at 1310(15) keV, which is not seen in the two-proton knockout spectrum.

The energy of the  $2_1^+$  state in  $^{66}\text{Fe}$  has been previously established at 573 keV by Hannawald *et al.* [15] in  $\gamma$ -ray spectroscopy following  $\beta$  decay of  $^{66}\text{Mn}$ . In the same experiment a candidate for the  $4_1^+ \rightarrow 2_1^+$  transition at 840 keV was proposed.

The transitions observed here at 571(6) and 567(6) keV in one- and two-proton knockout channel, respectively, are the most intensive ones and within experimental uncertainties they are in agreement with the 573-keV transition observed by Hannawald *et al.* We thus assume they correspond to the  $2_1^+ \rightarrow 0_{g.s.}^+$  transition in  $^{66}\text{Fe}$ . Further, the  $\gamma$ -ray observed here at 833 keV is in agreement with the  $4_1^+ \rightarrow 2_1^+$  transition tentatively proposed by Hannawald *et al.* at 840 keV.

The experimental statistics does not allow to draw any conclusions from study of  $\gamma$ - $\gamma$  coincidences. It is thus hard to propose assignments for the remaining transitions observed at 957 and 1310 keV. One of those may correspond to a  $6_1^+ \rightarrow 4_1^+$  transition. This supposition is based on the notion that spins of the two  $f_{7/2}$  holes can be coupled only to a total spin of 0, 2, 4, or 6 units of angular momentum. It is thus reasonable to

expect a population of the  $6_1^+$  excited state in a proton knockout experiment. This, however, does not exclude a possibility of population of nonyrast states. In fact, population of  $2_2^+$  states was observed in knockout reactions, e.g., in Ref. [28].

### B. $^{68}\text{Fe}$

Prior to this experiment no excited states in  $^{68}\text{Fe}$  were reported in the literature. Here, two transitions are clearly observed at 517(6) and 859(9) keV in the spectrum obtained in coincidence with  $^{68}\text{Fe}$  residues produced in one-proton knockout from  $^{69}\text{Co}$ . There is also a weak indication of a transition at 808(9) keV. The  $\gamma$ -ray spectrum resulting from coincidences with  $^{68}\text{Fe}$  produced in two-proton knockout has far fewer statistics and displays only an indication of a  $\gamma$  ray at the same energy as the most intense transition observed in the one-proton knockout spectrum. Because the 517 keV  $\gamma$ -ray is the most intense observed in coincidence with  $^{68}\text{Fe}$  residues we tentatively associate it with the  $2_1^+$  to the ground-state transition. The  $\gamma$  ray observed at 859 keV may correspond to the  $4_1^+ \rightarrow 2_1^+$  transition; however, similarly to the case of  $^{66}\text{Fe}$ , other assignment cannot be excluded.

### C. Inclusive two-proton knockout cross sections

In the present experiment an attempt was made to perform  $\gamma$ -ray spectroscopy of  $^{64}\text{Cr}_{40}$ . The intensities of secondary beams in the region of  $^{64}\text{Cr}$  available at existing fragmentation facilities do not allow for  $\gamma$ -ray spectroscopy with  $\beta$  decay or Coulomb excitation. We therefore examined the possibility of populating excited states in  $^{64}\text{Cr}$  by means of two-proton knockout from a fast secondary beam of  $^{66}\text{Fe}$  impinging on a thick secondary  $^9\text{Be}$  target.

The inclusive cross section for this reaction was measured at  $\sigma_{\text{inc}} = 0.13(5)$  mb. This small cross section combined with the intensity of the secondary  $^{66}\text{Fe}$  beam available at the time of the experiment has rendered any meaningful  $\gamma$ -ray spectroscopy unfeasible within the present work.

However, it is very interesting to compare the inclusive cross sections for all two-proton knockout reactions measured

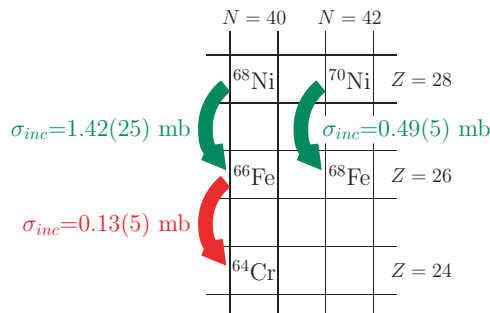


FIG. 5. (Color online) Two-proton knockout reactions and their inclusive cross sections as measured in this work. Note a striking difference in the cross section for reactions along  $N = 40$ .

in the same experiment in this region. As illustrated in Fig. 5, in addition to the  $^9\text{Be}(^{66}\text{Fe}, ^{64}\text{Cr})\text{X}$  reaction, two other two-proton knockout reactions were studied and their cross sections extracted:  $^9\text{Be}(^{68}\text{Ni}, ^{66}\text{Fe})\text{X}$  with  $\sigma_{\text{inc}} = 1.42(25)$  mb and  $^9\text{Be}(^{70}\text{Ni}, ^{68}\text{Fe})\text{X}$  with  $\sigma_{\text{inc}} = 0.49(5)$  mb. The order-of-magnitude drop in cross section for the reactions along the  $N = 40$  isotone line is striking.

It has been shown that the two-proton knockout from neutron-rich projectiles is predominantly a direct process [29]. The sequential process of one-proton knockout followed by the evaporation of a second proton from an intermediate nucleus is strongly hindered because the neutron separation threshold in a neutron-rich nucleus is in general much lower than the proton separation threshold. The reaction can thus be described as a sudden, direct process, involving only a limited number of degrees of freedom, a process in which two protons are removed from a projectile while the rest of nucleons remains essentially undisturbed. A reaction theory formalism, using eikonal dynamics and microscopic, correlated two-nucleon transition densities from shell-model calculations, has been developed recently [30,31]. The calculated two-nucleon amplitudes carry the nuclear structure details on the parentage and phase of the participating two-nucleon configurations in the ground state of the projectile with respect to the final states of the projectile-like reaction residue.

We can compare the experimental cross sections to those calculated from wave functions obtained from the GXPF1 interaction [32] in the  $fp$  model space for  $N = 40$ . The  $pf$  shell neutrons have a closed-shell configuration for  $N = 40$ . For  $Z = 28$  the GXPF1 interaction gives a large single-particle energy gap between the  $\pi f_{7/2}$  and  $\pi f_{5/2}, p_{3/2}$ , and  $p_{1/2}$  orbitals, and the proton wave functions for  $Z < 28$  are dominated by the  $\pi(f_{7/2})^n$  configurations. Following the formalism described in Ref. [31] the calculated partial cross sections for  $^9\text{Be}(^{68}\text{Ni}, ^{66}\text{Fe})\text{X}$  are 0.14, 0.45, 0.51, and 0.66 mb for final states with spins  $I^\pi = 0^+, 2^+, 4^+$ , and  $6^+$ , respectively, with an inclusive cross section of 1.76 mb. We have used the average quenching factor of  $R_S(2N) = 0.50$  obtained from the systematics discussed in Ref. [33]. This cross section is in reasonable agreement with the experimental value of 1.42(25). However, excitation energies for  $^{66}\text{Fe}$  obtained with GXPF1 of 0, 1.34, 2.14, and 2.48 MeV for  $0^+, 2^+, 4^+$  and  $6^+$  state, respectively, are not in overall agreement with experiment. The lower  $2^+$  energy observed in experiment is a clear signal that  $\nu(pf)^{n-2}(g_{9/2})^{+2}$  ( $n = 20$ ) configurations are important for the low-spin states. Thus, we should expect admixtures of  $\nu(pf)^n$  and  $\nu(pf)^{n-2}(g_{9/2})^{+2}$  in the spectrum of  $^{66}\text{Fe}$  with the calculated  $2N$  cross section split according to the amount of  $\nu(pf)^n$  component in the wave functions.

The calculated partial cross sections for  $^9\text{Be}(^{66}\text{Fe}, ^{64}\text{Cr})\text{X}$  are 0.19, 0.21, 0.23, and 0.30 mb for final states with spins  $I^\pi = 0^+, 2^+, 4^+$ , and  $6^+$ , respectively, with an inclusive cross section of 0.93 mb. The drop in cross section from 1.76 to 0.93 mb for the  $^{68}\text{Ni}$  and  $^{66}\text{Fe}$  projectiles, qualitatively comes from the  $f_{7/2}^2$  spectroscopic factors whose sum is given by the combinatorial factor  $p(p-1)/2$  with  $p = 8$  and  $p = 6$  for the number of valence protons. The calculated value for the  $^{66}\text{Fe}$  projectile is much larger than the experimental value of 0.13(5). The states of  $^{64}\text{Cr}$  will have admixtures of  $\nu(pf)^n$  and

$\nu(pf)^{n-2}(g_{9/2})^{+2}$  (plus perhaps even higher number of particle excited to  $g_{9/2}$ ). The cross section for a specific final state could be very small if the initial and final neutron configurations are different. But total calculated cross section of 0.93 mb should be obtained when summed over all final states. Thus, the observed small inclusive cross section indicates that most of the expected strength is going to levels that lie above the neutron decay threshold. The masses for these nuclei are not measured [the Audi-Wapstra extrapolation gives a value of  $S_n = 5.7(5)$  MeV].

It would be very interesting to measure the cross section to all final states, including those above the neutron decay threshold. It is, however, unclear whether such a measurement is feasible as it would require an ability to discriminate the  $^{63}\text{Cr}$  fragments produced directly in the  $2p1n$  removal from the  $^{66}\text{Fe}$  beam from the same  $^{63}\text{Cr}$  produced indirectly by one-neutron evaporation from  $^{64}\text{Cr}$ . In both cases, there would be the same particles in the final state and it is not clear what could be the unique signature of their origin. Even if the resulting free neutron could be effectively detected, its energy and direction of momentum vector in the laboratory frame in any case would not be much different from the energy and direction of momentum vector of the beam.

It is reasonable to expect that structural changes are taking place between nickel and chromium at  $N \approx 40$  related to the neutron shell gap at  $N = 40$ . It is generally accepted that the tensor force reduces the gap between the neutron  $pf$  shell and  $\nu g_{9/2}$  orbital as protons are removed from the  $f_{7/2}$  orbital and neutrons added to the  $f_{5/2}$  orbital [2,3,12]. As a result, appreciable occupancy of the  $\nu g_{9/2}$  orbital due to neutron pair scattering can be expected already for  $N < 40$ . The strength of the interaction and thus the magnitude of the gap reduction and  $\nu g_{9/2}$  occupancies are not precisely known.

A number of experimental studies on nickel, iron, and chromium isotopes with  $N \leq 40$  provide indirect evidence of this effect and suggest an increasing importance of the  $\nu g_{9/2}$  orbital already for  $N < 40$  as  $Z$  is reduced from 28 toward the middle of the  $\pi f_{7/2}$  shell [10,14–21].

An analogy might be drawn between the island of inversion near  $^{31}\text{Na}$  at  $N \approx 20$  and the region of neutron-rich chromium and titanium isotopes at  $N \approx 40$  [3,12,13]. In the island of inversion in the region of  $^{31}\text{Na}_{20}$ , the nuclear ground states are dominated by deformation-driving particle-hole  $2\hbar\omega$  intruder configurations of the type  $\nu(sd)^{-2}(fp)^{+2}$ . A somewhat similar phenomenon is expected to exist in the region of neutron-rich  $N \approx 40$  nuclei around  $^{62}\text{Ti}$  and  $^{64}\text{Cr}$  with the  $0\hbar\omega$  space consisting of the  $pf$  shell and  $2\hbar\omega$  intruder configurations in the  $sdg$  shell.

One may expect that the existence of such a new island of inversion would imprint a signature on the cross sections for direct reactions in the vicinity of the island and especially on reactions that cross the boundary of the island (i.e., with a projectile from outside of the island and a residue from within the island). Such a case has been recently studied by Gade *et al.* [33] with the two-proton knockout reaction  $^9\text{Be}(^{38}\text{Si},^{36}\text{Mg})\text{X}$ . The ground state of  $^{38}\text{Si}$  is well described within the  $0\hbar\omega$  space, whereas, prior to the experiment, the structure of the  $^{36}\text{Mg}$  was unknown. Small partial cross sections of  $\sigma(\text{g.s.}) =$

0.058(9) mb to the ground state and  $\sigma(2_1^+) = 0.042(8)$  mb to the first excited state of  $^{36}\text{Mg}$ , compared with much larger cross sections calculated theoretically with the model space restricted to  $0\hbar\omega$  configurations, led to the conclusion that the structure of low-energy states in  $^{36}\text{Mg}$  is dominated by intruder configurations. Thus,  $^{36}\text{Mg}$  has been placed within the island of inversion.

A similar, quantitative analysis is not yet possible in the region of  $N \approx 40$ . The realistic two-nucleon amplitudes cannot be computed due to the lack of a reliable shell-model Hamiltonian and also due to the large dimension of the required model space.

Following the arguments of Ref. [33] for the case of  $^9\text{Be}(^{38}\text{Si},^{36}\text{Mg})\text{X}$  two-proton knockout together with the predicted reduction of the gap between normal and intruder orbitals for  $N \approx 40$ ,  $Z < 28$  nuclei, the discrepancy between the experimental cross sections reported here and the one calculated for the  $pf$  model space seems to support, at least qualitatively, the hypothesis of significant differences in the amount of intruder configurations in the ground state and low-energy excited states of  $^{68}\text{Ni}$ ,  $^{66}\text{Fe}$ , and  $^{64}\text{Cr}$ . Certainly, more work, both on the theoretical and experimental sides, is necessary to verify this hypothesis and to gain further insight into the evolution of nuclear structure in this region.

#### IV. SUMMARY

In summary, in-beam  $\gamma$ -ray spectroscopy of neutron-rich  $^{66}\text{Fe}_{40}$  and  $^{68}\text{Fe}_{42}$  has been studied at the NSCL. These hard-to-reach nuclei have been produced and excited by means of one- and two-proton knockout at intermediate beam energy. The previous measurement of the  $E(2_1^+)$  and  $E(4_1^+)$  energy in  $^{66}\text{Fe}$  has been confirmed. In addition,  $\gamma$  rays at 957(10) and 1310(15) keV were observed in coincidence with  $^{66}\text{Fe}$ .

Prior to this experiment, no excited states in  $^{68}\text{Fe}$  were reported in the literature. Here, we observed a  $\gamma$  ray at 517(6) keV that we associate with the  $2_1^+ \rightarrow 0_{\text{g.s.}}^+$  transition in  $^{68}\text{Fe}$ . In addition, a  $\gamma$  ray at 859(9) keV is observed in one-proton knockout channel to  $^{68}\text{Fe}$ . There is also a weak indication of a transition at 808(9) keV.

The  $\gamma$ -ray spectroscopy of  $^{64}\text{Cr}$  was attempted. However, a surprisingly small inclusive cross section for the  $^9\text{Be}(^{66}\text{Fe},^{64}\text{Cr})\text{X}$  two-proton knockout reaction,  $\sigma_{\text{inc}} = 0.13(5)$  mb, was determined. It is suggested that this small cross section is an indication of intruder dominated low-energy structure of  $^{64}\text{Cr}$ . Advances in theory as well as in experiment are crucial to confirm this interpretation and to gain further insights into the evolution of nuclear structure in this region.

#### ACKNOWLEDGMENTS

This work was supported by US National Science Foundation under Grants PHY-0606007 and PHY-0555366 and by the United Kingdom Science and Technology Facilities Council (STFC) under Grant EP/D003628.

- [1] J. Dobaczewski, I. Hamamoto, W. Nazarewicz, and J. A. Sheikh, *Phys. Rev. Lett.* **72**, 981 (1994).
- [2] T. Otsuka, R. Fujimoto, Y. Utsuno, B. A. Brown, M. Honma, and T. Mizusaki, *Phys. Rev. Lett.* **87**, 082502 (2001).
- [3] B. A. Brown, *Prog. Part. Nucl. Phys.* **47**, 517 (2001), and references within.
- [4] J. Dobaczewski, N. Michel, W. Nazarewicz, M. Ploszajczak, and J. Rotureau, *Prog. Part. Nucl. Phys.* **59**, 432 (2007), and references within.
- [5] C. Thibault, R. Klapisch, C. Rigaud, A. M. Poskanzer, R. Prieels, L. Lessard, and W. Reisdorf, *Phys. Rev. C* **12**, 644 (1975).
- [6] X. Campi, H. Flocard, A. K. Kerman, and S. Koonin, *Nucl. Phys.* **A251**, 193 (1975).
- [7] E. K. Warburton, J. A. Becker, and B. A. Brown, *Phys. Rev. C* **41**, 1147 (1990).
- [8] Y. Utsuno, T. Otsuka, T. Glasmacher, T. Mizusaki, and M. Honma, *Phys. Rev. C* **70**, 044307 (2004).
- [9] T. Otsuka, T. Suzuki, R. Fujimoto, H. Grawe, and Y. Akaishi, *Phys. Rev. Lett.* **95**, 232502 (2005).
- [10] O. Sorlin *et al.*, *Phys. Rev. Lett.* **88**, 092501 (2002).
- [11] K. Langanke, J. Terasaki, F. Nowacki, D. J. Dean, and W. Nazarewicz, *Phys. Rev. C* **67**, 044314 (2003).
- [12] T. Otsuka, T. Matsuo, and D. Abe, *Phys. Rev. Lett.* **97**, 162501 (2006).
- [13] O. Sorlin *et al.*, *Eur. Phys. J. A* **16**, 55 (2003).
- [14] R. Grzywacz *et al.*, *Phys. Rev. Lett.* **81**, 766 (1998).
- [15] M. Hannawald *et al.*, *Phys. Rev. Lett.* **82**, 1391 (1999).
- [16] O. Sorlin *et al.*, *Nucl. Phys.* **A669**, 351 (2000).
- [17] M. Sawicka *et al.*, *Eur. Phys. J. A* **16**, 51 (2003).
- [18] S. J. Freeman *et al.*, *Phys. Rev. C* **69**, 064301 (2004).
- [19] L. Gaudefroy *et al.*, *Eur. Phys. J. A* **23**, 41 (2005).
- [20] A. N. Deacon *et al.*, *Phys. Lett.* **B622**, 151 (2005).
- [21] N. Aoi, *J. Phys.: Conf. Ser.* **49**, 190 (2006).
- [22] N. Hotelling *et al.*, *Phys. Rev. C* **74**, 064313 (2006).
- [23] S. Zhu *et al.*, *Phys. Rev. C* **74**, 064315 (2006).
- [24] D. J. Morrissey, B. M. Sherrill, M. Steiner, A. Stolz, and I. Wiedenhoever, *Nucl. Instrum. Methods B* **204**, 90 (2003).
- [25] D. Bazin, J. A. Caggiano, B. M. Sherrill, J. Yurkon, and A. Zeller, *Nucl. Instrum. Methods B* **204**, 629 (2003).
- [26] W. Mueller, J. A. Church, T. Glasmacher, D. Gutknecht, G. Hackman, P. G. Hansen, Z. Hu, K. L. Miller, and P. Quirin, *Nucl. Instrum. Methods A* **466**, 492 (2001).
- [27] *GEANT3 - Detector Description and Simulation Tool*, CERN Program Library Long Writeup W5013 (CERN, Geneva, 1993).
- [28] K. Starosta *et al.*, *Phys. Rev. Lett.* **99**, 042503 (2007).
- [29] D. Bazin *et al.*, *Phys. Rev. Lett.* **91**, 012501 (2003).
- [30] J. A. Tostevin, G. Podolyák, B. A. Brown, and P. G. Hansen, *Phys. Rev. C* **70**, 064602 (2004).
- [31] J. A. Tostevin and B. A. Brown, *Phys. Rev. C* **74**, 064604 (2006).
- [32] M. Honma, T. Otsuka, B. A. Brown, and T. Mizusaki, *Phys. Rev. C* **65**, 061301(R) (2002).
- [33] A. Gade *et al.*, *Phys. Rev. Lett.* **99**, 072502 (2007).